

## **Guidelines for the geometry design of local microseismic arrays**

Zuolin Chen

### **ABSTRACT**

Error analysis of hypocenter location provides an efficient method for the design of local microseismic monitoring arrays. By using the equation of the error ellipsoid derived from the conventional generalized inverse method at a 3-D grid system in the study area, the hypocenter error contour mapping of a space containing a local microseismic monitoring array and its vicinities was drawn. As the technique provides the error distribution of a planning array before construction, it can be used to preview and examine whether the alignment of the stations can satisfy the need of precision in the object areas, and provide the evidence for further adjustments of the array. Also, through a series of numerical experiments, some rules of array design are derived, and these rules provide the theoretical evidence and guidelines for the design and optimization of local microseismic monitoring arrays.

### **INTRODUCTION**

The effect of the configuration of seismic arrays upon the hypocenter location error has long been an important issue in seismology. Analyzing the accuracy of hypocenter location for a planned seismic array can not only provide error estimations but also save many deployment and maintenance costs. For an existing seismic array, a rapid, convenient and accurate acquisition of error analysis can also provide theoretical guidelines for further improvement of the array.

The usual approach for error analysis is to calculate standard errors of the hypocenter parameters for each solution obtained by a least-squares inversion procedure assuming random picking errors in the arrival time data (Flinn, 1965; Evernden, 1969; Jordan and Sverdrup, 1981). This conventional generalized inverse method of locating local events from P and/or S arrival times employs an iterative linearized inversion of a system of equations that relate travel time residuals to adjustments of calculated hypocenter location. A Monte Carlo procedure, which involves perturbing the arrival times with random errors and relocating the event, is an alternate approach for error analysis (Billings et al., 1994). However, this method is generally inconvenient, extremely time-consuming, and difficult to apply for the calculation of events in such a large scale 3-D grid.

Generally, the accuracy of the hypocenter location of microseismic events with a local array depends on the accuracy of the assumed velocity model used to generate travel times, the array geometry, and the inherent accuracy of the arrival times used (Peters and Crosson, 1972). The sources of error presented in arrival times can be divided into two categories of random and systematic errors (Billings et al., 1994). The random error is mainly induced by the picking error of arrival times, and the systematic error is caused by the difference between the assumed and real velocity models. The systematic error in hypocenter location arising from an inadequate assumed velocity model is unknown and fixed with a geometry and choice of phases. In a small extent like a local seismic array,

the effect of the systematic error on location is generally neglected. Thus, in the following error analysis, only the random source of travel time error will be considered.

In this study, we finished a computer program to calculate the size of the error ellipsoid at the nodes of a 3-D grid system. Based on the calculated maximum horizontal and vertical errors of location in a series of 2-D horizontal cross sections (depth slices) which depict the errors in difference spatial positions can be derived. By comparing the error distribution through adjusting the configuration, scale, number of stations, azimuthal gap and depth gap of local arrays, a variety of regularities associated with the array design are confirmed. These regularities become the guidelines for the geometry design of local passive microseismic monitoring arrays.

## METHODOLOGY

### Hypocenter location method

A conventional hypocenter location procedure seeks to find a hypocenter which minimizes the difference between the observed and calculated arrival times by using a least-squares method. The characteristic function is

$$SSR = \sum_{i=1}^N (t_i^{obs} - t_i^{cal}(\theta(x, y, z, t_o)))^2 \quad (1)$$

where  $t_i^{obs}$  denotes the observed arrival times at station  $i$ ,  $t_i^{cal}$  the corresponding calculated arrival time, and  $N$  the number of stations. To determine the estimate  $\theta_e(x_e, y_e, z_e, t_{0e})$  of hypocenter parameters  $\theta$ , one usually starts from an initial guess  $\theta_0(x_0, y_0, z_0, t_{00})$ .

Often through several iterations the updated  $\theta^{(n+1)} = \theta^{(n)} + \Delta\theta^{(n)}$  will reduce the value of the  $SSR$  characteristic function to a predefined criterion. At each iterative step,  $\Delta\theta^{(n)}$  is calculated by fitting the linearized model of

$$r^{(n)} = A(\Delta\theta^{(n)})^T \quad (2)$$

where  $r^{(n)}$  denotes the residual vector of  $(t^{obs} - t^{cal})$  for  $\theta^{(n)}$ ;  $A$  is the  $N \times M$  matrix of partial derivatives of  $t$  with respect to the  $M$  components of  $\theta$  at iteration  $n$ ;  $(\Delta\theta^{(n)})^T$  is the transpose of vector  $\Delta\theta^{(n)}$ .

For clarity, the extensions of  $A$  and  $\Delta\theta^{(n)}$  are given as follows:

$$A = \begin{pmatrix} \partial x_1 / \partial t & \partial y_1 / \partial t & \partial z_1 / \partial t & 1 \\ \partial x_2 / \partial t & \partial y_2 / \partial t & \partial z_2 / \partial t & 1 \\ \cdot & \cdot & \cdot & \cdot \\ \partial x_N / \partial t & \partial y_N / \partial t & \partial z_N / \partial t & 1 \end{pmatrix} \quad (3)$$

$$\Delta \theta^{(n)} = \left( \Delta x^{(n)} \quad \Delta y^{(n)} \quad \Delta z^{(n)} \quad \Delta t_0^{(n)} \right) \quad (4)$$

The elements of  $r^{(n)}$  and matrix  $A$  are often weighted by assigned standard deviations  $\sigma_i$ .

We seek the least-squares solution which best solves equation (2) in the sense of minimizing  $(r^{(n)} - A(\Delta \theta^{(n)})^T)^2$ . This can be done by pre-multiplying by  $A^T$  (transpose of  $A$ ) to get the least-squares condition

$$\Delta\theta^{(n)} = (A^T A)^{-1} A^T w_i r^{(n)} \quad (5)$$

where  $w_i$  are the weighting factors and often assumed to be inversely proportional to the distance between the station and hypocenter. Equation (5) is often called the normal equation, and the solution can be sought in terms of generalized inverse of matrix  $A$ .

### Error ellipsoid

To determine the expected error of the location, the error ellipsoid is often calculated to depict the error distribution. The error ellipsoid computation is based on the theory of Flinn(1965) and Everden(1969). This method has been widely used by many well-known hypocenter location algorithms like HYPOINVERSE (Klein, 1978).

Based on the mentioned theory, the points  $\theta_p(x_p, y_p, z_p, t_{0p})$  on the  $p\%$  confidence ellipsoid for the solution  $\theta_e(x_e, y_e, z_e, t_{0e})$  is obtained from

$$(\theta_p - \theta_e)^T Q (\theta_p - \theta_e) \leq \kappa_p^2, \quad (6)$$

where  $Q=(A^T A)^{-1}$ , the parameter covariance matrix. The confidence coefficient  $\kappa_p^2$  depends on the confidence coefficient (Draper and Smith, 1966; Rowlett and Forsyth, 1984),

$$\kappa_p^2 = Ms^2 F(p; M, N - M) \quad (7)$$

where  $F(p; M, N-M)$  is the  $F$  distribution with  $M$  and  $N-M$  degrees of freedom at the  $p\%$  confidence level.  $M$  is the number of unknown parameters of hypocenter location and is equal to 4;  $N$  is the number of stations. The variance factor,  $s^2$ , is a *posterior* estimate of the unknown variance of picking error of arrival times of seismic phases ( $\sigma^2$ ) and is estimated from

$$s^2 = \frac{1}{(N - M)} \left( \sum_{i=1}^N w_i r_i^{(n)} \right)^2 \quad (8)$$

Based on this information, the semi-axes of the error ellipsoid can be obtained from the eigenvalues of  $Q$  by using the singular value decomposition (SVD) method, that is

$$R_i^{semi} = \sqrt{s^2 \text{eigenvalue}_i} \sqrt{2F(p; 4, N - 4)} \quad (9)$$

## NUMERICAL EXPERIMENTS

The research purpose of the numerical experiments is to examine the problem that if an observation array is deployed, what is the hypocenter location error in the entire study area of interest? Given we want to add extra stations in several accessible locations, where should they be placed? To solve these problems, we start to observe the effect of array design from a 5-station square array pattern on the location accuracy. Several other related array configurations were developed for the examination of their effects on the accuracy of location.

### Pre-conditions of the numerical experiments

In particular, a constant velocity model (with P-wave velocity  $V_p=4000$  m/s) was chosen in this study. The constant-velocity model has the advantages of simplicity, and ease of interpretation and comparison of results from various array configurations. All stations are placed at zero elevation except in the last section where the effect of depth gap of stations is discussed.

As the prior data variance ( $\sigma^2$ ) of picking error is assumed to be known beforehand in the numerical experiments, there is no need to estimate the posterior variance factor  $s^2$  from the travel time residuals  $r_i^{(n)}$  in equation (8).

The standard picking error of P-arrivals (that is,  $\sigma_i$ ,  $i=1$  to  $N$ ) is assumed to be a function of hypocentral distance of an event to a station ( $D_i^{epi}$ ). It increases with  $D_i^{epi}$  as a step function as follows:

$$\begin{aligned} \sigma_i &= 0.001 \text{ sec} && (D_i^{epi} \leq D_{max}^{array}/2); \\ \sigma_i &= 0.002 \text{ sec} && (D_{max}^{array}/2 < D_i^{epi} \leq D_{max}^{array}); \\ \sigma_i &= 0.004 \text{ sec} && (D_i^{epi} > D_{max}^{array}); \end{aligned}$$

where  $D_{max}^{array}$  is the maximum lateral interval between stations of an array in either easting or northing.

The variable standard picking error also functions as a kind of weighting factor, which enhances the effect of nearby stations and reduces the effect of distant ones.

Every event is recorded at all stations though the assumption is not required in real hypocenter location procedures.

In numerical experiments, as the assumed velocity model to create the synthetic travel data of events and that used for relocation of the events are the same, systematic error caused by velocity model is removed. Thus the picking error will be the only source of the input error.

To produce the error contour maps and plot error ellipses, events are aligned on a grid with a spacing of 100 meters in both easting and northing. Errors in both horizontal and depth directions are viewed by introducing a series of horizontal parallel horizontal cross

sections (depth slices) with a spacing interval of 100 meters in depth. The surface where stations are usually deployed is regarded as the zero depth reference level. To simplify the question, events on the nodes of the grid are assumed to be relocated back to their original positions.

### **The error distribution based on a five-station square array geometry**

Firstly, the error distribution of a simple 5-station square array geometry provides the essential control which geometry exerts and the symmetry for the reference of other configurations. Four stations are located on the corners of the square with a spacing of 1000 meters in both northing and easting. An extra station is aligned in the center of the square. The reason to add a station at the center of the square is due to the fact that the station number must be larger than the four unknown factors to acquire a stable  $F$  distribution. For convenience in the later descriptions, some major geometric areas of the array are named Figure 1.

Figures 2a and 2b illustrate the distributions of the one-standard-error (68%) ellipses along the horizontal cross sections from shallow to deep. The major features of the distributions of the horizontal errors are as follows: errors are smaller within the array and increase with distance to the center of the array; errors along the horizontal slices always increase with depth; the long axes of each error ellipse shows a tendency to radiate from the center of the array. Similarly, vertical errors are smaller within the frame of the array, and the smallest area exists close to the center of the array. Another feature of distributions of the vertical errors is that in the areas close below the stations, errors tend to be smaller than those in the surrounding areas. This tendency becomes weaker with depth. In contrast to the variation of horizontal errors with depth, the trend of the vertical errors is to decrease to a certain depth and then to increase again.

The above features are easier to identify when the error distributions are plotted into contour maps (Figures 2c and 2d). From the maps, we can see the maximum horizontal errors can be restrained to 10m-20m close to the center and to 40m in most areas within the frame of the array when the depth of the horizontal cross section is less than 550m or approximately half of the side length of the array. Outside the frame of the array, the errors increase from 100m to 300m downwards. On the other hand, the maximum vertical error can be controlled to 40m close to the center, and to 100m in most areas within the frame when the depth of the horizontal cross section is less than approximately half of the side length of the array. It seems that the maximum vertical errors within the frame are largest in shallow, decrease gradually to the depth of 550m (half of the side length of the array) and then turn to increase again. Outside the array, the vertical errors show a similar variation patterns with depth as those inside the array. For convenience, from now on, we will omit the word “maximum” in front of the terms of “maximum horizontal errors” and “maximum vertical errors”.

It should be noted that a station can dramatically reduce both horizontal and vertical errors in its vicinity on the shallow cross sections. This appearance blurs with the increase of depth of the cross sections.

As the contour maps provide information for the analysis of the errors qualitatively and quantitatively, we will mainly use these instead of the error ellipses to describe errors in the following parts.

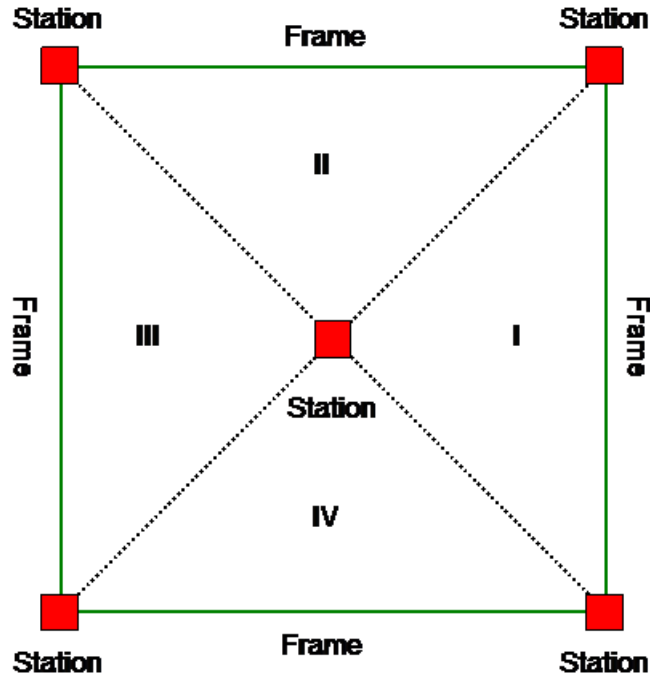


Figure 1. Illustration of the names of some major geometric areas for later descriptions. Red solid squares are stations; I,II,III and IV are four quadrants within the array. Lines (solid green) outlining the array are called the frame.

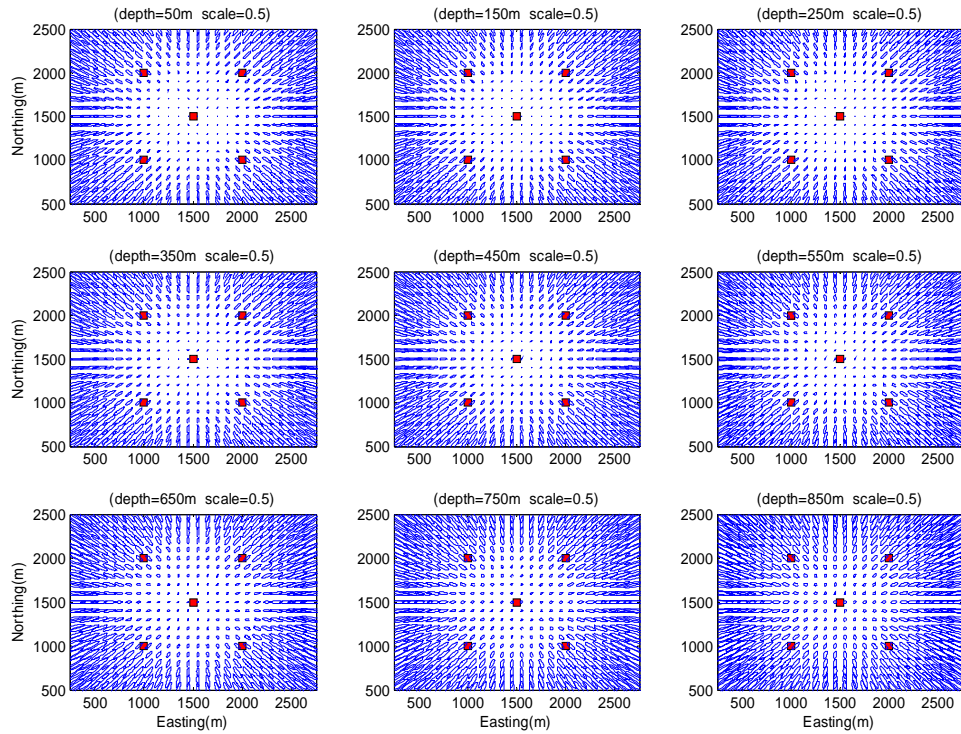


Figure 2a. Horizontal cross-sections of the horizontal projections (northing-easting) of error ellipsoids located by using a 5-station square array. The stations are denoted by red solid squares; Error ellipses in the sections are plotted in blue lines. The spacing of assumed events is 100 meters in both northing and easting.

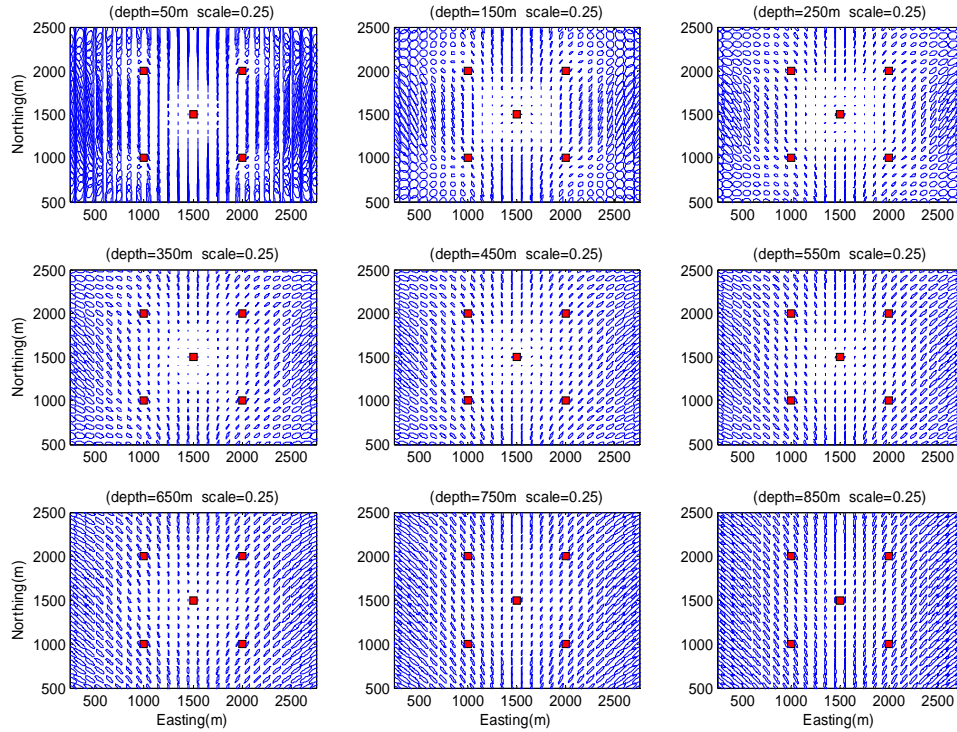


Figure 2b. Horizontal cross sections of the vertical projections (easting-depth) of error ellipsoids located by using a 5-station square array. The stations are denoted by red solid squares; Error ellipses in the sections are plotted in blue lines. The spacing of assumed events is 100 meters in both northing and easting.

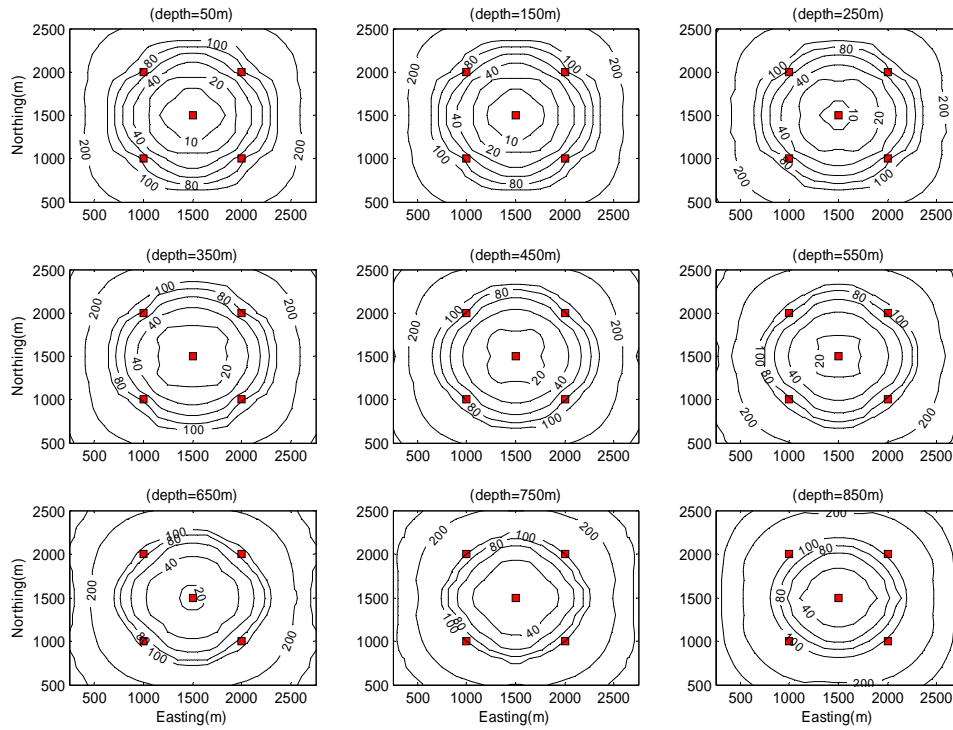


Figure 2c. Horizontal error contour maps for the 5-station square array. Constant velocity  $V_p=4000$  m/s. The contour values are variable, with 10, 20, 40, 60, and 80 meters below the 100-meter contour and a constant 100 meter interval above the contour. Stations are marked by solid squares and their depth are zero meters. Depths of the horizontal cross sections are marked on the top of each picture.

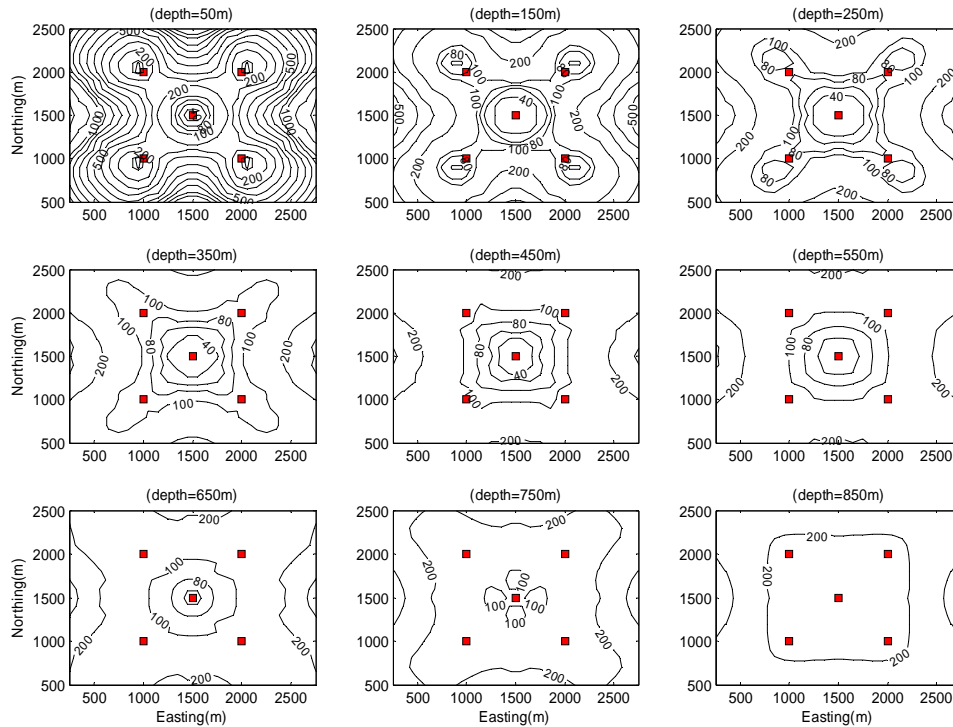


Figure 2d. Contour maps of the vertical error located by using a 5-station square array. The side length of the square is 1000 meters. Depths of the horizontal cross sections are marked on the top of each picture. Similar to Figure 2c.

### The effects of the scale of an array on error distributions

To observe the effect of the scale of an array on errors, the error distributions based on a smaller 5-station square array with a side length of 600m are calculated (Figures 3a and 3b). The patterns of the contour maps are generally similar to the corresponding maps in the previous larger 1000m square array except the error values.

Compared to the results of the previous larger array, the horizontal errors are generally larger both inside and outside of the array. Similarly, when the depths are approximately less than approximately half of the side length of the array (see the horizontal cross section at 350m depth), the horizontal errors are roughly restrained to 10m-20m when close to the center and to 40m within the frame. However, beyond this depth, horizontal errors located by the smaller array are often approximately 2-3 times larger both inside and outside of the array even at the same depth.

The vertical errors located by the small 600m array are generally worse, as are the horizontal errors. Again, for the same depth, compared to the larger array, vertical errors are 2-3 times larger both inside and outside the array in the study area.

The appearance that a nearby station reduces both horizontal and vertical errors in the shallow depths can also be identified. It blurs with the increase of depth of the cross sections as well.

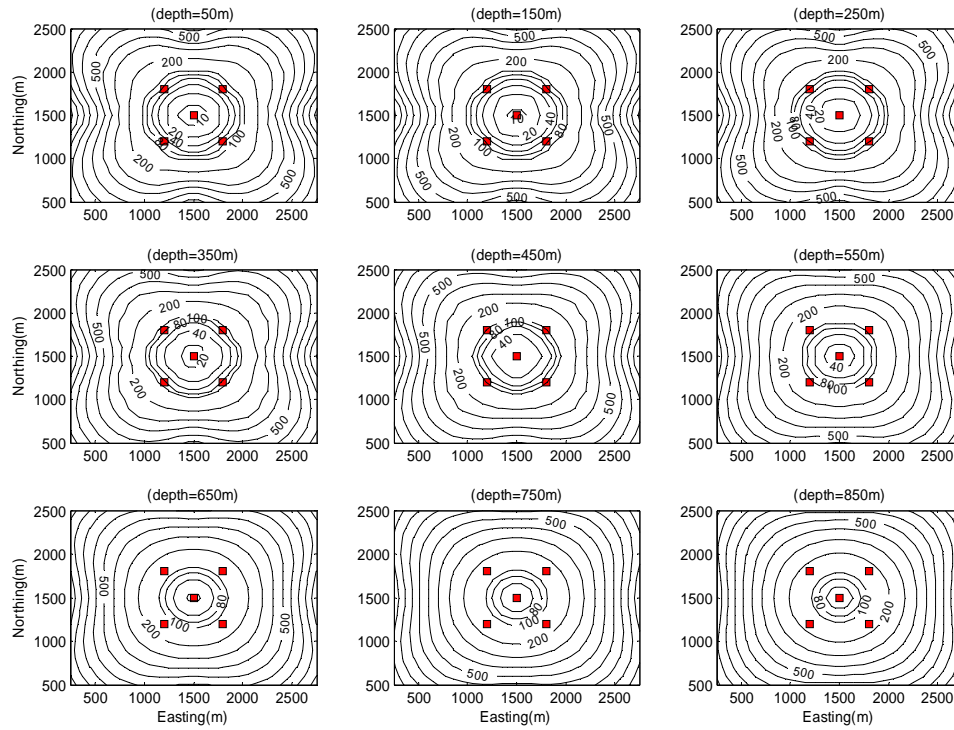


Figure 3a. Contour maps of the horizontal error located using a 5-station square array. The side length of the square is 600 meters. Depths of the horizontal cross-sections are marked on the top of each picture.

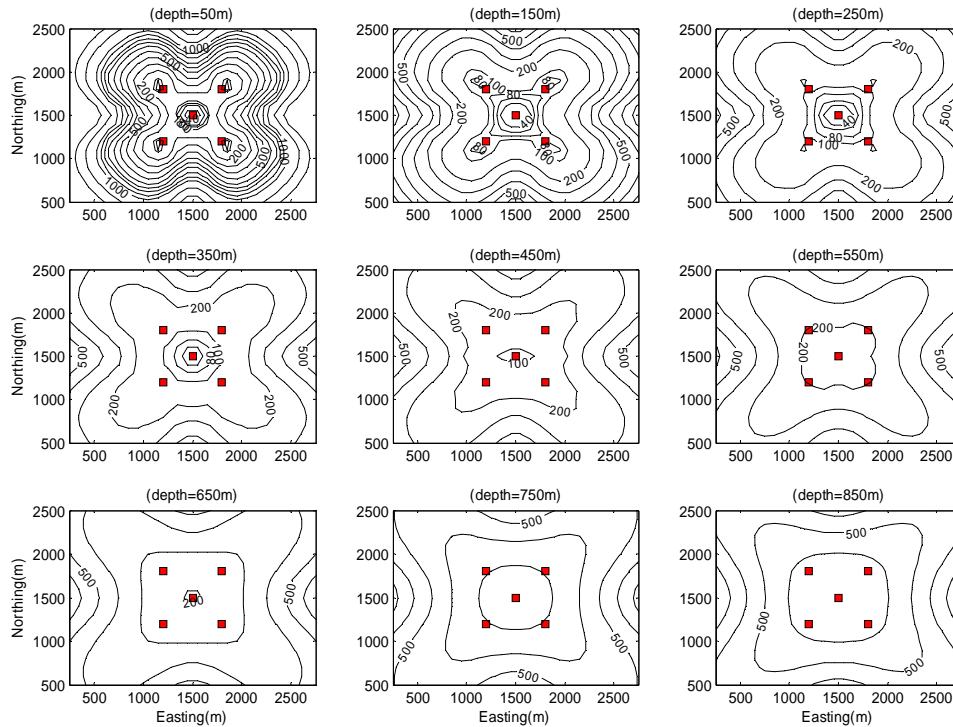


Figure 3b. Contour maps of the vertical error located using a 5-station square array. The side length of the square is 600 meters. Depths of the horizontal cross sections are marked on the top of each picture.

### The effect of the number of stations

From experience, location errors generally decrease with the increase of the number of stations. As the construction of new stations in a given seismic array is often costly and sometimes impossible, the effect of adding various numbers of stations should be considered seriously beforehand. In the following sections, we present three examples to show the effects of different cases by adding one and *many* stations to the proceeding 5-station square array.

In the case of adding only one station to the square array (now six-station), the horizontal errors in the areas close to newly-added stations are dramatically reduced in different depths (Figure 4a and 4b). The errors are also reduced to approximately 10m close to the center of the array. The effect of adding the new station on the vertical error is more obvious: it reduces the errors 100m to several hundred meters in the vicinity throughout the study depth and area. At a depth of 850m, the errors in the entire study area are reduced to approximately 100m.

To test the effect of adding *many* stations, we added an additional five and eight stations with arbitrary positions within the frame on the basis of the proceeding six-station array separately. As a result of adding five stations to the array, the 10m-contour for the horizontal errors is expanded to the whole frame of the array when the cross section is shallower than 250m; the 60m-contour increases to the size of the 100m-

contour located by the six-station array at the depth of 850m (Figure 4c and 4d). Generally, compared to the six-station array, the vertical errors are further reduced by approximately 50% using *many* stations. Results from adding eight stations to the array show that, although the total errors are further reduced, the effects are not so dramatic as in the improvement between adding one and five new station (Figures 4e and 4f).

To summarize, by adding *many* stations within an array, both horizontal and vertical errors can be consistently reduced, especially in the vicinity of the newly added stations. The accuracy of estimated location increases with the number of stations. However the relationship between the accuracy and the number of stations seems not to be linear, and its effect tends to slow down after adding a certain number of stations to the 5-station array.

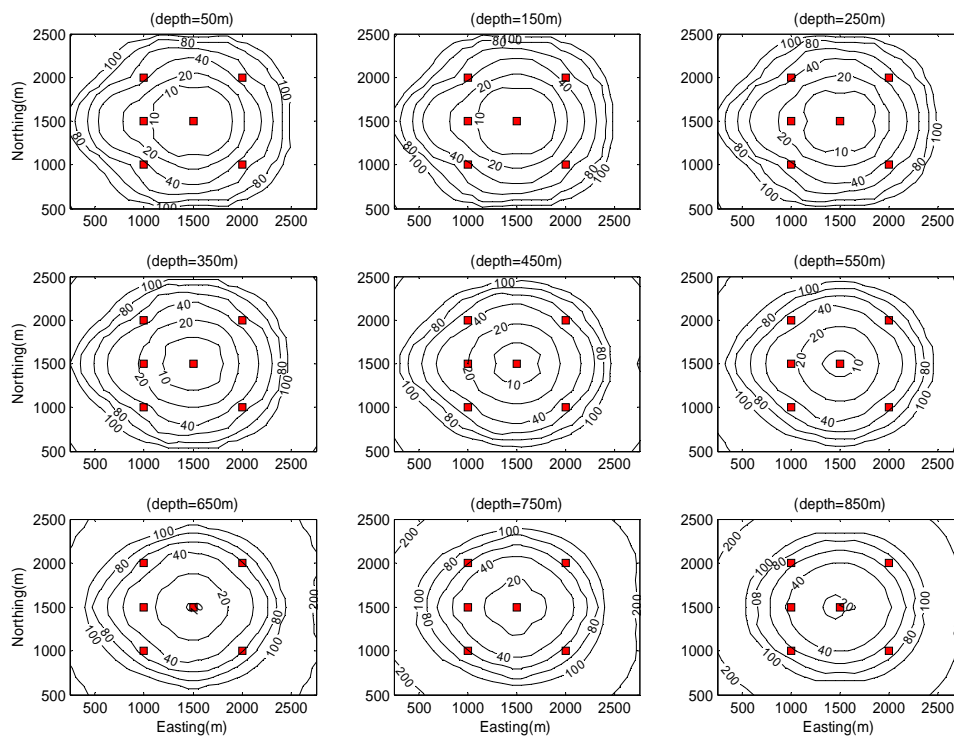


Figure 4a. Contour maps of the horizontal error obtained by adding an additional station to the preceding 5-station square array on the left frame.

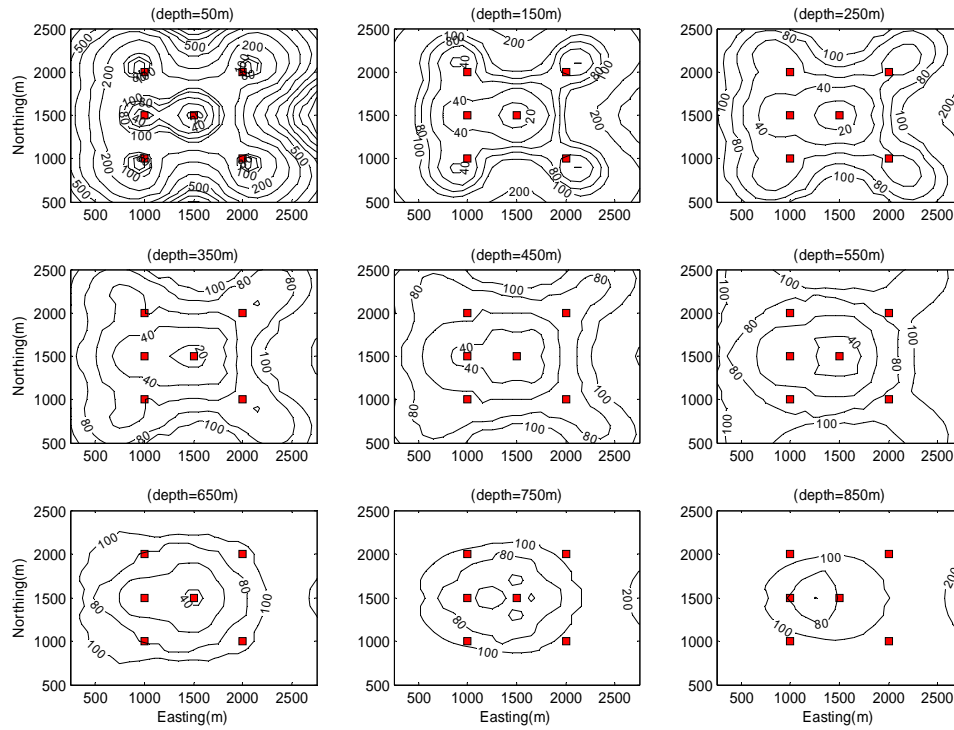


Figure 4b. Contour maps of the vertical error obtained by adding an additional station to the preceding 5-station square array on the left frame.

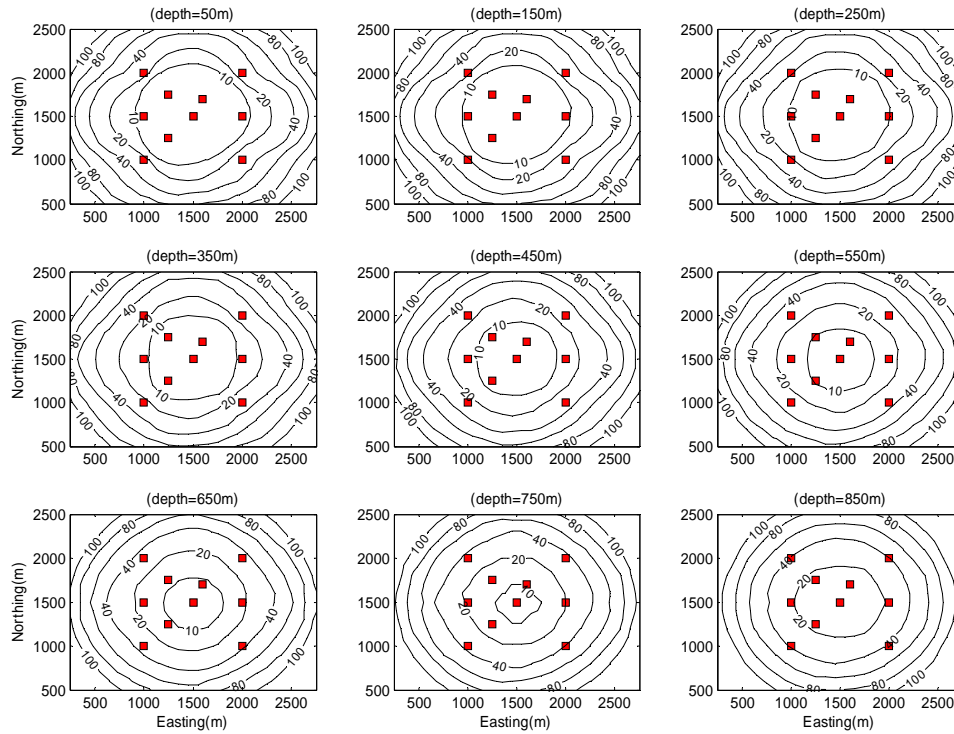


Figure 4c. Contour maps of the horizontal error obtained by adding five additional stations arbitrarily to the preceding 5-station square array on the left frame.

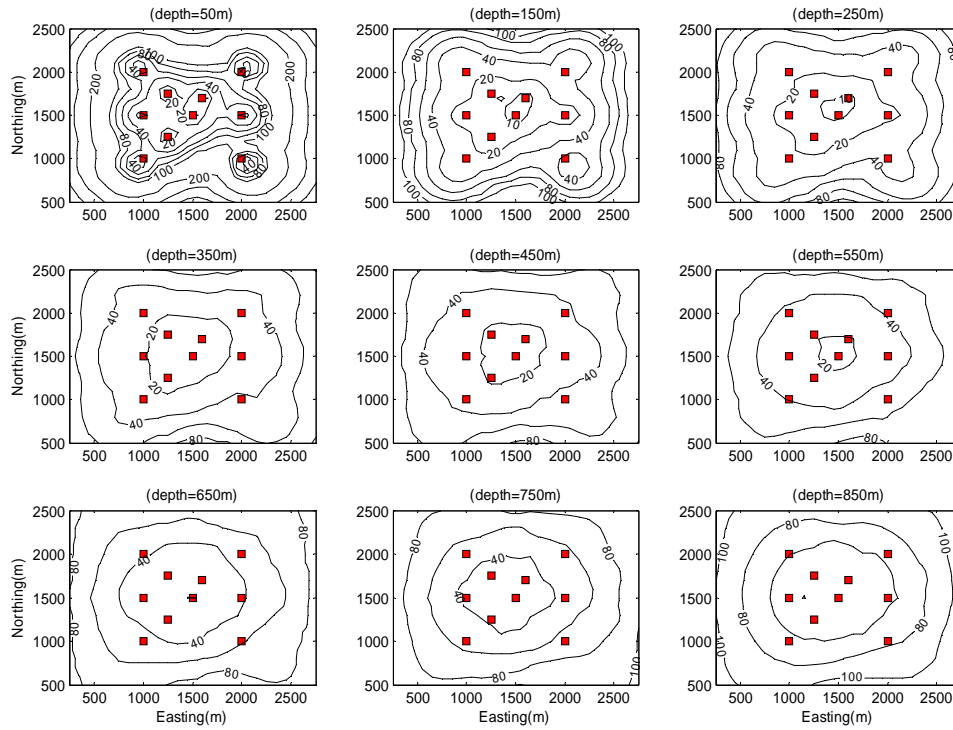


Figure 4d. Contour maps of the vertical error obtained by adding five additional stations arbitrarily to the preceding 5-station square array on the left frame.

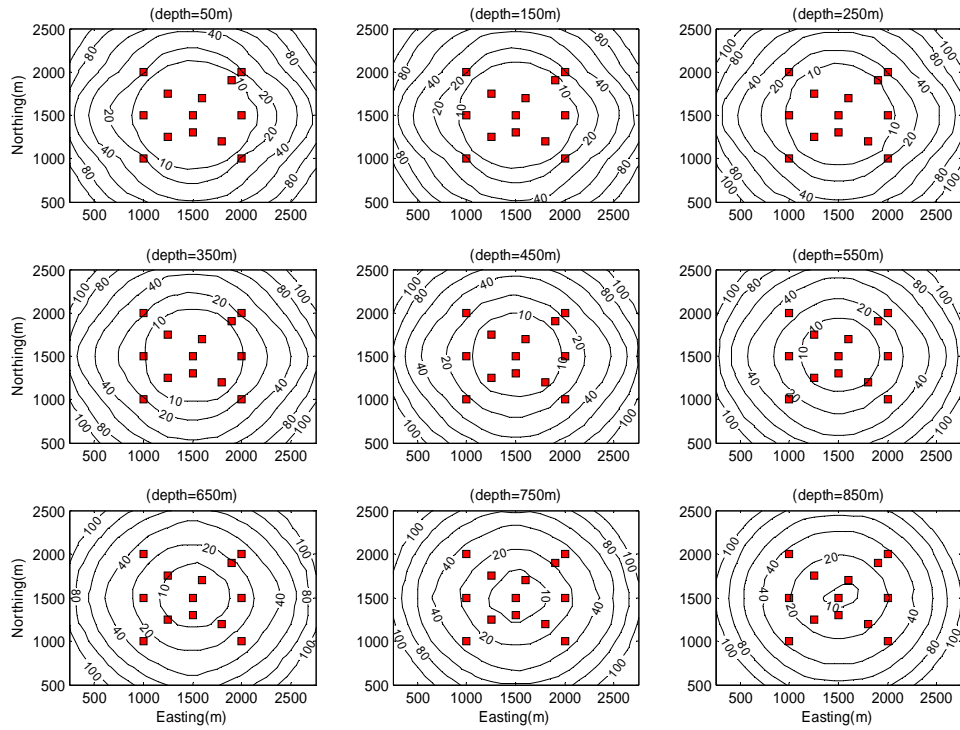


Figure 4e. Contour maps of the horizontal error obtained by adding eight additional stations arbitrarily to the proceeding 5-station square array on the left frame.

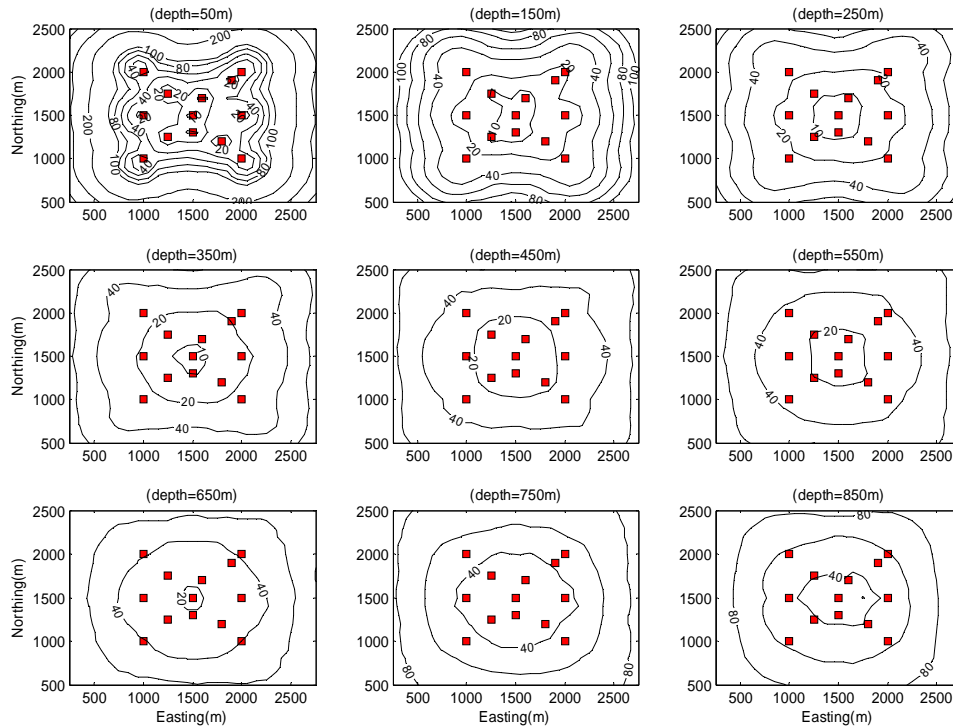


Figure 4f. Contour maps of the vertical error obtained by adding eight additional stations arbitrarily to the proceeding 5-station square array on the left frame.

### The effects of the azimuthal gap of stations on error distributions

Azimuthal gap of stations has been regarded as one of the several crucial factors that affecting detection capability. The definition of azimuthal gap is the largest angle between two adjacent stations as viewed from an event. The effect of the azimuthal gap of station on errors is examined using an array in which events in its four symmetric quadrants (see Figure 1) have different azimuthal gaps even though their locations are equivalent in each quadrant. Among the four quadrants, events occurring in Quadrant I tend to have the smallest general azimuthal gaps, Quadrant II and IV have intermediate gaps, and Quadrant III the largest.

As a result, it is obvious that both horizontal and vertical errors are smaller within the quadrant with smaller azimuthal gap or more stations along its long side (Figure 5a and 5b); In other words, errors tend to be larger when the azimuthal gap increases. This appearance blurs with the increase of the depth.

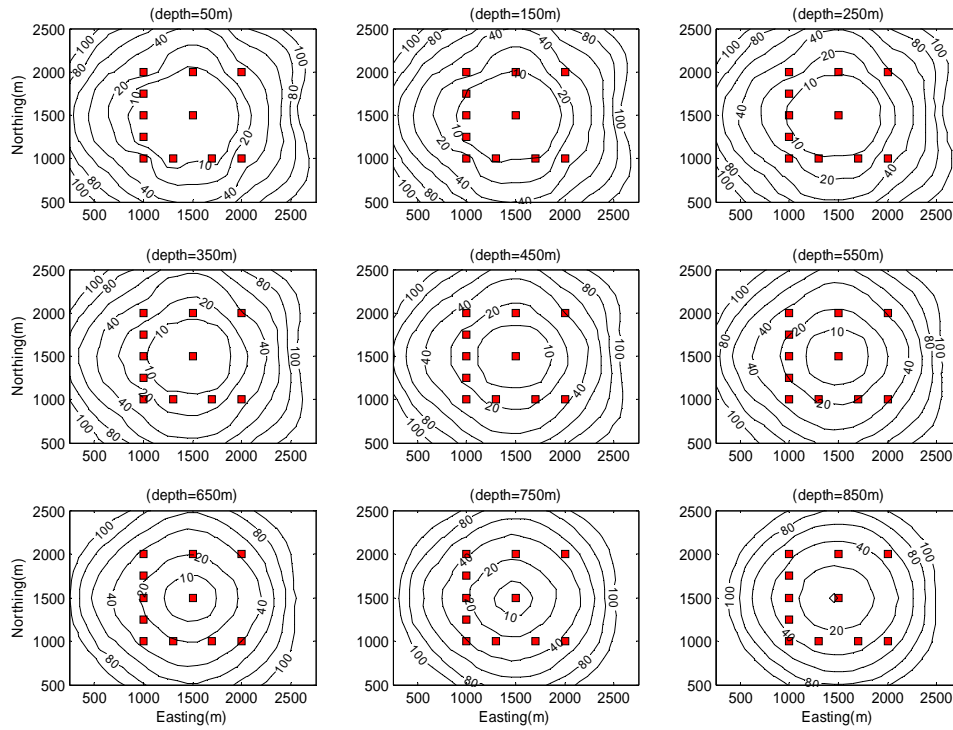


Figure 5a. Contour maps of the horizontal error obtained using an array with four kinds of azimuthal gaps in the four quadrants (see Figure 1).

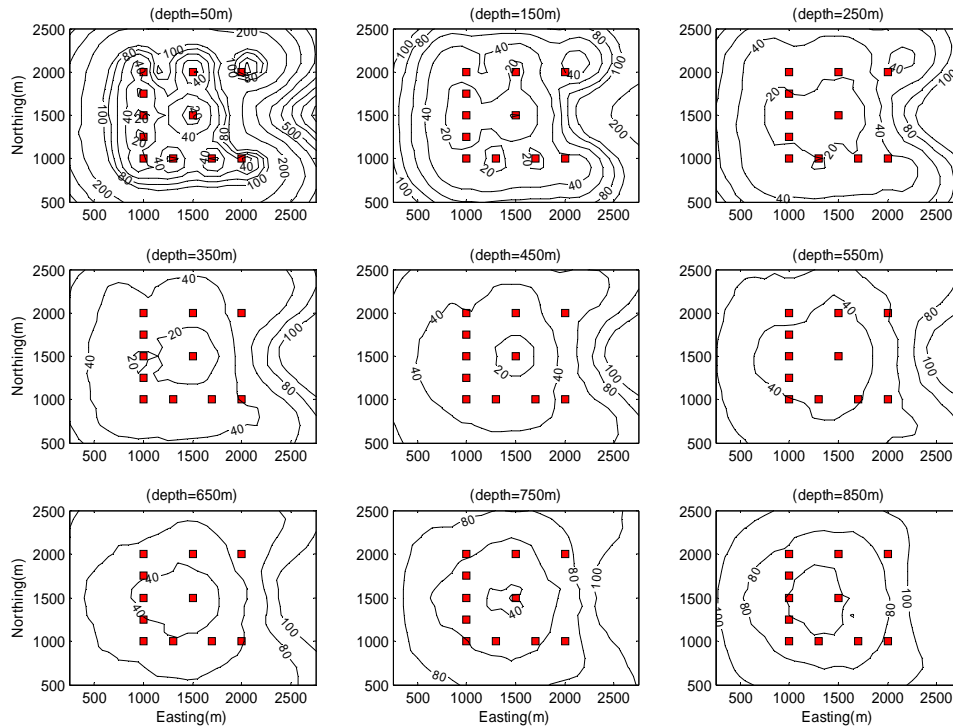


Figure 5b. Contour maps of the vertical errors obtained using an array with four kind of azimuthal gaps in the four quadrants (see Figure 1).

### The effect of the depth gap of stations

The results in the previous sections are derived under the assumption that all stations are located on the surface with the same elevation levels. Some effects of a 3D-like array on the resolution of the hypocenter location are examined and compared using two examples of 5-station square arrays with different depth gaps.

The first example is an array with a small depth gap, with the station in the center of the array 50 m higher than the other four corner stations. The second example is similar to the first except the depth gap is increased to 100 m.

Figures 6a and 6b show the errors of the first array with a 50-meter depth gap. Compare with the 5-station square with all stations on the same elevation levels (Figure 2a-2d), it can be seen that the horizontal errors are reduced approximately 50% at shallow depth. However, the effect declines with increasing depth.

Similar to the horizontal errors, vertical errors are mainly reduced at shallow depth. The effect of the depth gap to the accuracy of location decreases with the increase of the depth. The only difference between the error distributions of the 50m and 100m depth gap arrays is that the appearance found in the latter is more obvious (Figures 6c and 6d). Hence, we speculate that a 3-D array with a small depth gap between stations could improve the accuracy of location, especially in the shallow subsurface. This appearance becomes more obvious with increase of the depth gap of an array.

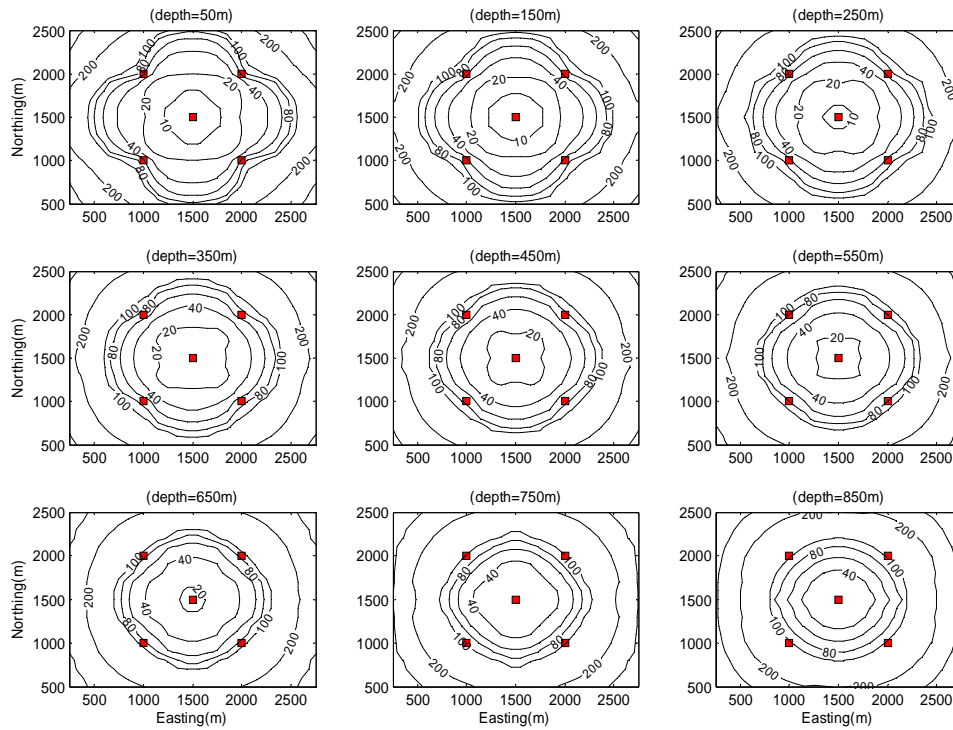


Figure 6a. Contour maps of the horizontal error located by a square 5-station array with the station in the center 50 meters higher than the four corner stations.

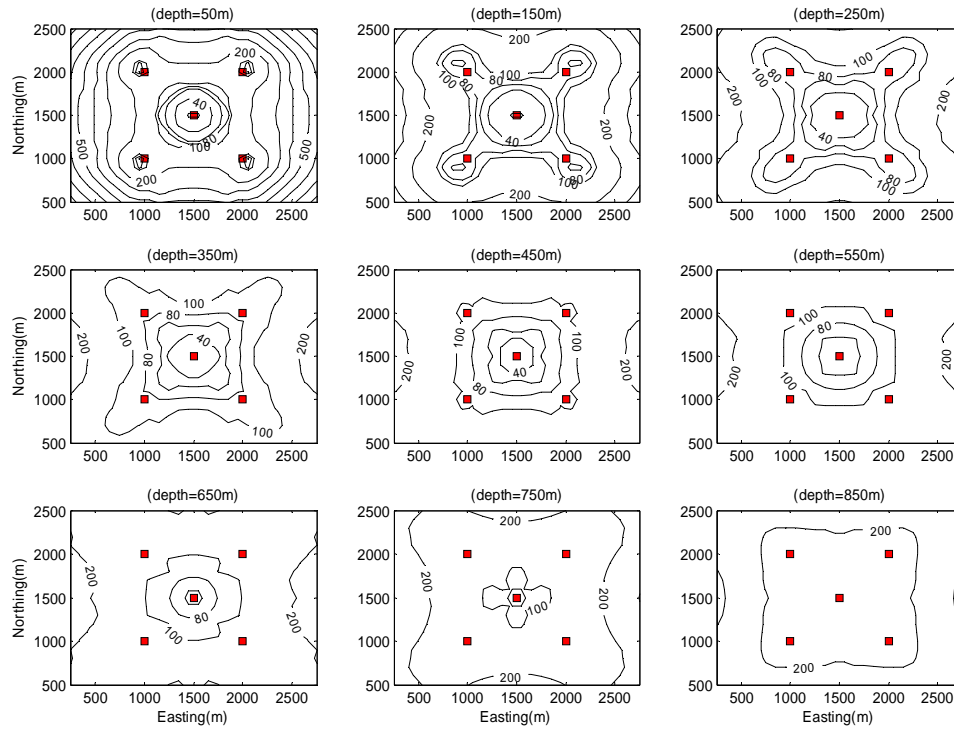


Figure 6b. Contour maps of the vertical error obtained using a square 5-station array with the station in the center 50 meters higher than the corner stations.

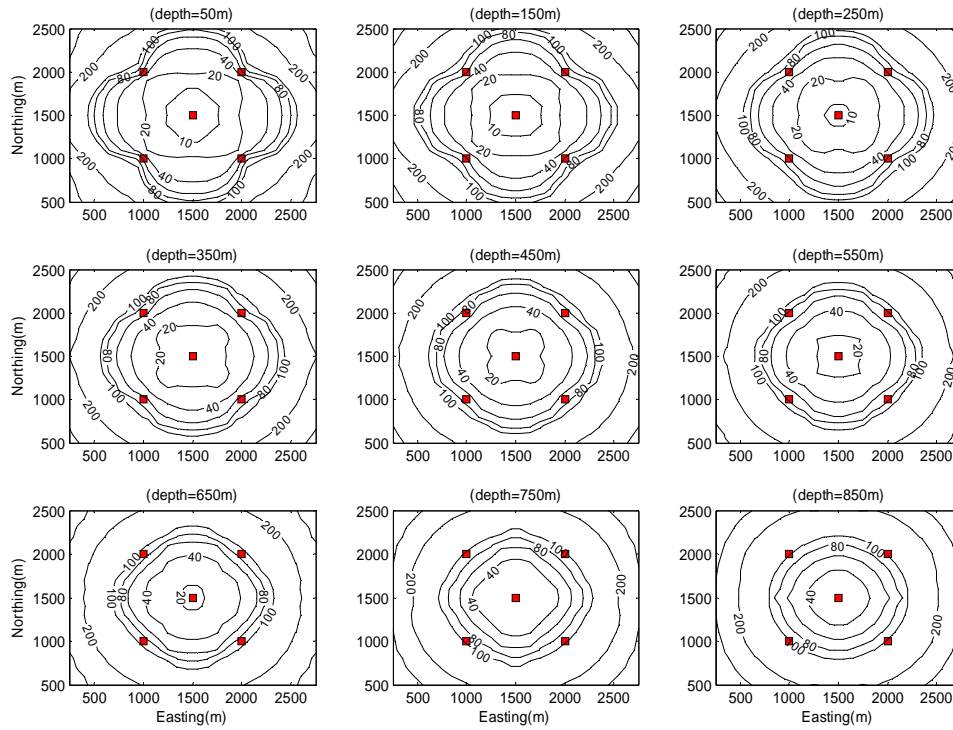


Figure 6c. Contour maps of the horizontal error obtained using a square 5-station array with the station in the center 100 meters higher than the corner stations.

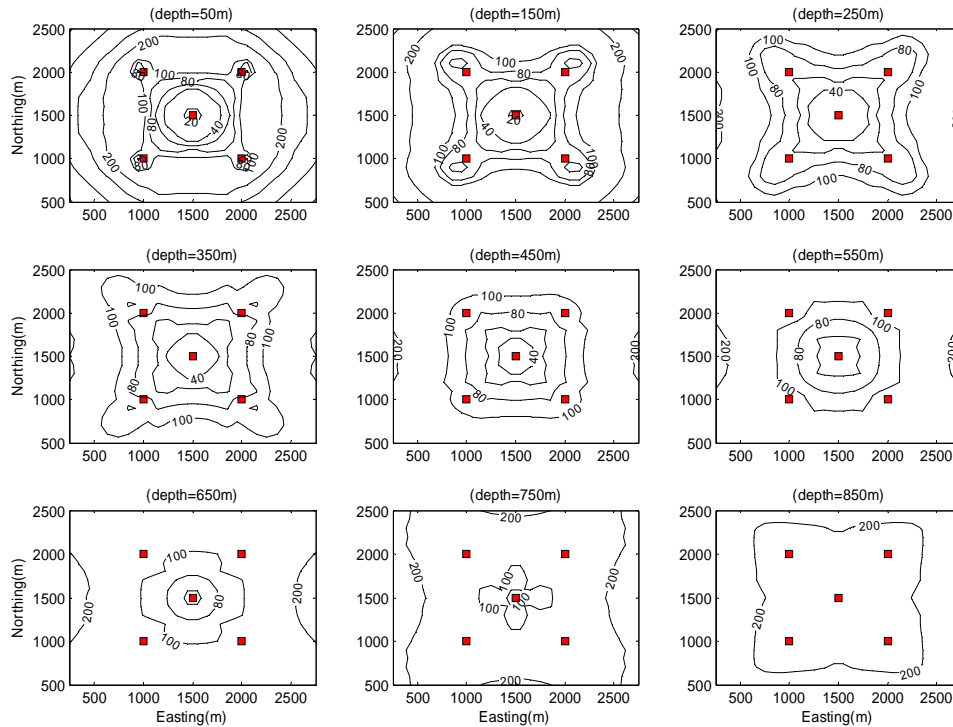


Figure 6d. Contour maps of the vertical error obtained using a square 5-station array with the station in the center 100 meters higher than the corner stations.

## CONCLUSIONS

We have demonstrated many important relationships between the distribution of stations of an array and the hypocenter location error using the one-standard confidence error ellipses and the corresponding contours derived from the solution of normal equation through a series of numerical experiments. The relationships form the basis for guidelines for the design of local seismic arrays. In conclusion, we summarized the previous regularities as follows:

The horizontal errors are generally smaller inside the frame of an array, and tend to be smallest in the vicinity of the center; outside the array, errors increase rapidly. The constraint of an array on the horizontal errors is better close to the elevation level of the array, and becomes weaker with increasing depth.

Similar to the horizontal errors, vertical errors tend to be smaller inside the frame of an array and smallest in the vicinity of the center; Outside of the array, error increases dramatically with distance to the array. One distinct difference between these two kinds of errors is that the smallest error cross section does not appear close to the elevation level of the array; the general vertical errors seem to decrease downwards to a certain depth and start to increase after that depth. The depth of the cross section with smallest errors is approximately half of the side length of an array.

The scale of an array affects the accuracy of hypocenter location a great deal. Horizontally, although both the patterns and values of horizontal and vertical errors inside the frame are in equivalent levels within a certain depth (approximately half of the side length of an array), outside the frame errors increase much faster than those located by a larger one. Vertically, when the depth exceeds a certain depth, errors obtained using a smaller array also increase much faster than those determined by the larger one.

The accuracy of hypocenter location generally improved with the increase of the number of stations. A newly-added station within the frame of an array can greatly reduce the errors in the vicinity and affect the distant areas to some degree. *Many* newly-added stations within the array can improve the total performance of the array horizontally and vertically, inside and outside of the frame.

The examination of how the accuracy of hypocenter location is affected by the azimuthal gap of stations shows that both horizontal and vertical errors decrease within the areas with smaller azimuthal gaps. However, this appearance blurs with increasing depth.

A slight depth gap of stations in depth direction can improve the accuracy of location, especially in the shallow subsurface. This appearance is more obvious with an increase in the depth gap. Again, the appearance blurs with increasing depth.

### ACKNOWLEDGEMENTS

We thank the industrial sponsors of *CREWES* for their funding assistance.

### REFERENCES

- Billings S.D., Sambridge M.S. and Kennett B.L.N., 1994, Errors in hypocenter location: picking, model, and magnitude dependence: Bulletin of the Seismological Society of America, **84**, No.6, 1978-1990.
- Draper N.R. and Smith H., 1966, Applied Regression Analysis, 184-273, John Wiley, New York.
- Evernden J.F., 1969, Precision of epicenters obtained by small numbers of world-wide stations, Bulletin of the Seismological Society of America, **59**, No.3, 1365-1398.
- Flinn E.A., 1965, Confidence regions and error determinations for seismic event location: Rev.Geophys. **3**, No.1, 157-185.
- Jordan T.H. and Sverdrup K.A., 1981, Teleseismic location techniques and their application to earthquake clusters in the south-central pacific: Bulletin of the Seismological Society of America, **71**, No.4, 1105-1130.
- Klein F., 1978, Hypocenter location program HYPOINVERSE, U.S.Geol.Surv., Open-File Rept. 78-694, 1-113.
- Peters D.C., and Crosson R.S., 1972, Application of prediction analysis to hypocenter determination using a local array, Bulletin of the Seismological Society of America, **62**, No.3, 775-788.
- Rowlett H. and Forsyth D.W., 1984, Recent faulting and microearthquakes at the intersection of the Vema fracture zone and the Mid-Atlantic Ridge: J.G.R., **89**, No. B7, 6079-6094.